Anisotropic Validation of Hexahedral Meshes for Composite Materials in Biomechanics

Matthias Müller–Hannemann*
Friedrich-Wilhelms-Universität Bonn

Cornelia Kober**
Freie Universität Berlin

Robert Sader††
Technische Universität München

Hans-Florian Zeilhofer††
Technische Universität München

Abstract

We use a concrete simulation scenario to study the effect of hexahedral mesh size and mesh quality on the accuracy of the solution of a finite element analysis (FEA). Our test cases stem from biomedical research. We investigate a composite two-material model of a piece of bone from the human mandible on which we simulate a bite. In particular, we are interested whether material properties (soft vs. hard and isotropic vs. anisotropic) have a significant impact on the accuracy which can be achieved for the different kind of meshes.

We constructed hexahedral meshes of varying size, with an increasing number of elements in the neighborhood of the external force of our load case. For the hexahedral mesh generation, we used the iterative cycle elimination method of the first author together with squared condition number based optimized smoothing.

In this paper, we focus on the deformation as the post-processing variable. In our experiments, it seems that the solution of the FEA converges relatively fast with an increasing number of elements.

Our methodology to investigate the influence of the mesh quality on several post-processing variables is a systematic variation of the mesh quality by means of a controlled perturbation of an optimized mesh with a fixed mesh topology. The influence of mesh quality on the analysis results turns out to be relatively small. Even the mesh of poorest quality is within a range of not more than four percent from the results of our best quality mesh.

Concerning the analysis of a possible interdependence between numerical behavior and material law, we observed that the fully anisotropic (and so the most realistic) case shows also the best numerical behavior.

Keywords: hexahedral mesh generation, mesh quality, optimized mesh smoothing, FEM simulation, human mandible

1 Introduction

Over the years the finite element analysis (FEA) has become an increasingly important and generally accepted means in engineering for a wide variety of application areas. As Tautges [Tau01] has pointed out recently, the mesh generation research community has matured and specialized in the last years, but also moved away from the FEA side, and therefore, closer links between the mesh generation community and analysis communities must be re-established.

This paper is an initial attempt in this direction for a concrete application scenario with a two-material workpiece in the field of biomechanics. We consider three basic questions for all-hexahedral meshes:

1. How many hexahedral mesh elements are required to get meaningful results?
2. How important is mesh quality for the accuracy of the simulation?
3. Can we observe a different behavior of the convergence with respect to the degree of anisotropy?

The motivation for the first question is the hope that it might be feasible to work with meshes which can be handled on current PC's and which allow to realize short analysis times on such machines. Hence, we want to

*Dr. Matthias Müller-Hannemann, Rheinische Friedrich-Wilhelms-Universität Bonn, Forschungsinstitut für Diskrete Mathematik, Lennéstr. 2, 53113 Bonn, Germany, muellerh@or.uni-bonn.de; www.math.tu-berlin.de/~mhannema.

**Dr. Cornelia Kober, Freie Universität Berlin, Institut für Mathematik II, WE2, Arnimallee 2-6, 14195 Berlin, Germany, ckober@math.fu-berlin.de.

††PD Dr. Dr. Robert Sader, PD Dr. Dr. Hans-Florian Zeilhofer, Klinik und Poliklinik für Mund-Kiefer-Gesichtschirurgie der Technischen Universität München, Ismaninger Str. 22, 81675 München, Germany.

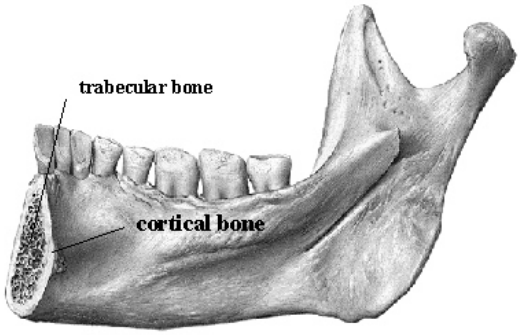

Figure 1: The bone structure of the human mandible (from [PP94, VO00]).

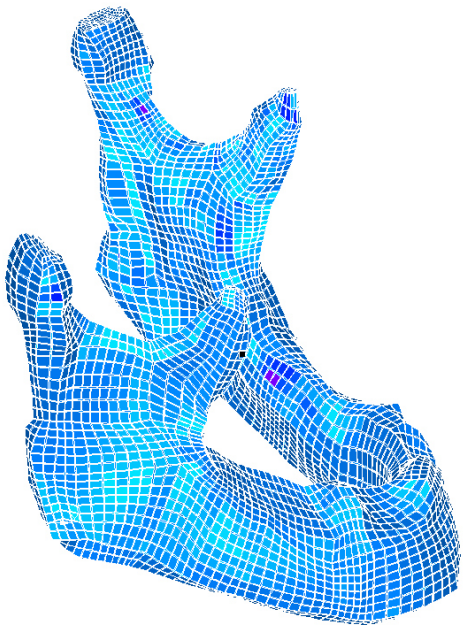

Figure 2: A hexahedral mesh for an individual shape of a human mandible from [KMH01].

give experimental support or to falsify that relatively small meshes can give *qualitatively* accurate results (in the sense that the solution and post-processing variables are in the correct order of magnitude).

There has been recent and quite remarkable progress with optimized mesh smoothing [Knu00], but these advanced routines are computationally expensive. As finding all-hexahedral meshes for complex domains is still a challenge, and as it is often hard — even with optimized smoothing — to find good-quality meshes we are interested in the second question.

Application background: Composite materials. The technological progress with composite materials, for example with fiber reinforced or layered media, offers a lot of new possibilities. Increasing demands in the analysis of more complex materials, for instance in lightweight construction, require increasingly sophisticated simulation techniques. Therefore FEA techniques have to keep up with these developments. To this end, a systematic evaluation of simulation capacities of inhomogeneous and anisotropic material behavior is required.

A very modern application is the FEA in the field of biomechanics. Simulations of the human femur or the tibia do have already some kind of "tradition", but newer research tends to more complex bony organs like the human mandible or even to soft tissue simulation.

In general, simulation in structural mechanics requires a representation of the specimen's geometry, the load case, and an appropriate material description. In contrast to the advanced stage of individual geometry reconstruction based on computed tomography data (CT data), the possibilities of a satisfying - individual - material description are still rudimentary. In this context, the inherent material is bone tissue, which is one of the strongest and stiffest tissues of the body. Bone itself is a highly complex composite material. Its mechanical properties are anisotropic, heterogenous and visco-elastic. The CT data give a density representation, however, the three-dimensional information about the anisotropic material law is lost. Most previous simulations in the field of biomechanics base on an isotropic and homogenous material law.

At a macroscopic scale, two different kinds of bone can be distinguished. *Cortical* or compact bone is present in the outer part of bones, while *trabecular*, *cancellous* or *spongious bone* is situated at the inner, see Figure 1. In case of long bones, trabecular bone is only present at the joints in the epiphyseal region, while for short and flat bone, it is encountered in the entire inner volume. The latter is also applicable for the human mandible and the maxilla, see for instance [MBS98, VO00].

From the point of simulation, not only the demand of a more or less acceptable material resp. geometry description is actual, but mainly its interplay and its combined influence on the significance of the simulation results.

The scope of this work is an analysis of the impact of our mesh generation techniques in combination with different material settings.

In order to concentrate on this purpose, we tried to eliminate any influence of individual shape, see Figure 2, and,

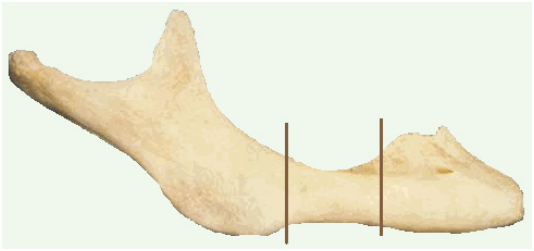

Figure 3: A piece of bone extracted from a toothless mandibular corpus.

therefore, restricted ourselves to an "artificial" piece of bone, done by parametric CAD. Concerning the shape, we oriented on a toothless mandibular corpus (Figure 3). For it is impossible to capture really the shape of biological tissue by parameterization, we tried to build it in the sense of an "envelope" of the original shape. In return, we can vary the "individual" material properties from the totally isotropic simplification as used in most of the simulations, to a fully anisotropic and inhomogeneous material description. We can additionally vary the shape. By that, also special investigations of the influence of the age-related corticalis' thickness become possible.

This research is part of a detailed simulation project concerning the human mandible. In previous publications [KST$^+$00, KBZ$^+$00], descriptions of the simulation concept have been given.

Overview. The rest of the paper is organized as follows. In Section 2 we give a brief description of the meshing techniques used to generate pure hexahedral meshes with different local mesh density. Then, in Section 3 we explain the underlying mathematical model of our simulation test cases. Section 4 studies the effect of the number of hexahedral elements to the solution accuracy with respect to the varying degrees of anisotropy across ten different test cases. Furthermore, we describe and evaluate an experiment which considers the impact of mesh quality on the accuracy of the solution obtained in the simulation. Finally, in Section 5, we summarize the main features of our approach and give directions for future work.

2 Hexahedral Mesh Generation Techniques for a Composite Model

Input model. The shape of our workpiece is represented by parameterized external and internal surface patches (*macro elements*). As mentioned in the Introduction, we

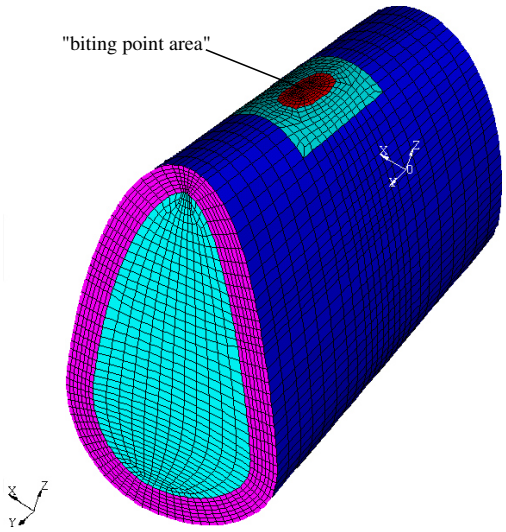

Figure 4: Surface mesh of the pice of bone.

want a comparison between meshes of different size with a local refinement in the neighborhood of the biting point. Such a comparison is only meaningful if we can guarantee to have exactly the same load case. The latter implies that we had to fix the load case regions for all meshes used in our experiments. This has been achieved by an appropriate addition and modification of the original macro elements.

Surface meshing. To guarantee conformal meshes for a more–than–one–component model, we first fix the quadrilateral surface mesh before we start the hexahedral meshing. The macro element mesh of a composite model possesses *branchings*, i.e. edges to which more than two elements belong. Conformal quadrilateral mesh refinement can be achieved in a robust way by first solving a certain system of linear equations and applying network flow techniques afterwards [MM00]. This method allows a tight local mesh density control which we used systematically to vary the mesh density in several ways. In particular, we changed the mesh density

1. locally in a neighborhood of the biting point area,
2. in the relatively thin surrounding component (the corticalis part),
3. with respect to the curvature (higher curvature requires finer meshes), and

4. along the longitudinal axis.

Hexahedral meshing techniques. For a recent survey on hexahedral mesh generation techniques for assembly geometries see [Tau01].

Given our surface meshes, the interior component (spongiosa part of the bone) is fairly easy meshable with sweeping techniques.

The local refinement near the biting point, however, yields a non-sweepable component. To mesh this component, we used the iterative cycle elimination method of the first author [MH99, MH01]. Recent advances with the cycle elimination scheme and the construction process to cope with local refinements (the insertion of internal sheets), as described in [KMH01], were crucial for the success of this method.

Afterwards, the mesh components are untangled and smoothed with optimization methods as suggested by Knupp and Freitag & Knupp [Knu00, FK99]. More precisely, we optimized with respect to the sum of the squared condition numbers as the objective function (as explained in detail in [KMH01]).

Figure 5 gives several views on details of a hex mesh with 30516 hexahedra for the piece of bone. Furthermore, in Figure 6 we show hexahedral meshes of different refinement levels.

3 Mathematical Model of the Simulation

Up to a strain limit of 0.3%, the material behavior of bone can be described by linear elasticity. In most physiological standard situations, this value is not exceeded.

Therefore, in the governing equation of structural mechanics $div(\sigma) = 0$, we apply for the stress tensor σ and the strain tensor ϵ a *generalized Hooke's law* which can be written in compressed notation as

$$\sigma_i = C_{ij}\,\epsilon_j,$$

where both i and j assume the values 1–6 and j is understood to be summed over these values. By symmetry relations, the 36 coefficients C_{ij} simplify to 21 independent values which are known as the *elastic constants*. In most materials, this number is further reduced. In *isotropic* materials, which behave the same in every direction e.g. steel, there are only two independent elastic constants. For highly anisotropic materials like bone, the number of elastic constants is between 2 and 21. Most anisotropic materials do exhibit some symmetry to their internal structure. Two common types of limited anisotropy happen to

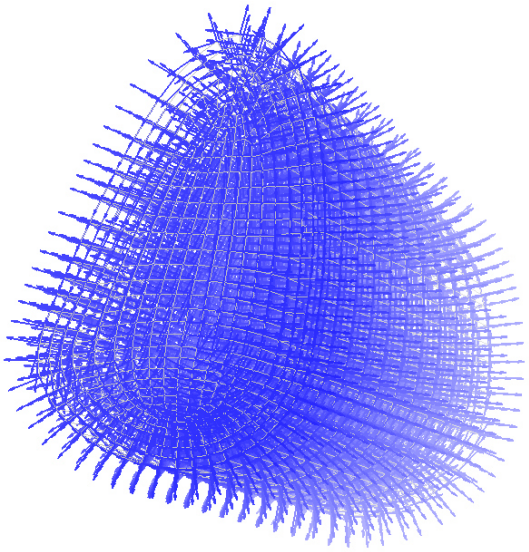

Figure 7: Principal directions of the elastic tensor.

be found in bone, wood and other biological tissue: The mechanical properties of *orthotropic* materials are different in three perpendicular directions, e.g. in axial, radial and circumferential direction, see Fig. 7. Their matrix of elasticity has nine independent values and the following form:

$$C = \begin{pmatrix} C_{11} & C_{12} & C_{13} & 0 & 0 & 0 \\ C_{12} & C_{22} & C_{23} & 0 & 0 & 0 \\ C_{13} & C_{23} & C_{33} & 0 & 0 & 0 \\ 0 & 0 & 0 & C_{44} & 0 & 0 \\ 0 & 0 & 0 & 0 & C_{55} & 0 \\ 0 & 0 & 0 & 0 & 0 & C_{66} \end{pmatrix}.$$

In the preceding paragraph, attention was directed to the use of the matrix C of the elastic constants, which is more amenable to analysis. Traditionally, material response has been characterized by "engineering" or "technical" constants. According to custom, the *Young modulus* E is used to describe the ability of a material to transfer a pure extensional strain into a pure extensional stress. The *Poisson ratio*, ν, is used to indicate the extent to which the lateral dimensions of a body decrease (or increase) in response to a pure extensional (or compressional) strain. The *shear modulus* G is used to describe the ability of a material to transfer pure shear strain into pure shear stress [Daw76]. In the anisotropic case, all these constants become direction dependent, so we have E_1, E_2, E_3 instead of E, $\nu_{ij}, G_{ij}, 1 \leq i, j \leq 3$ instead of ν and G.

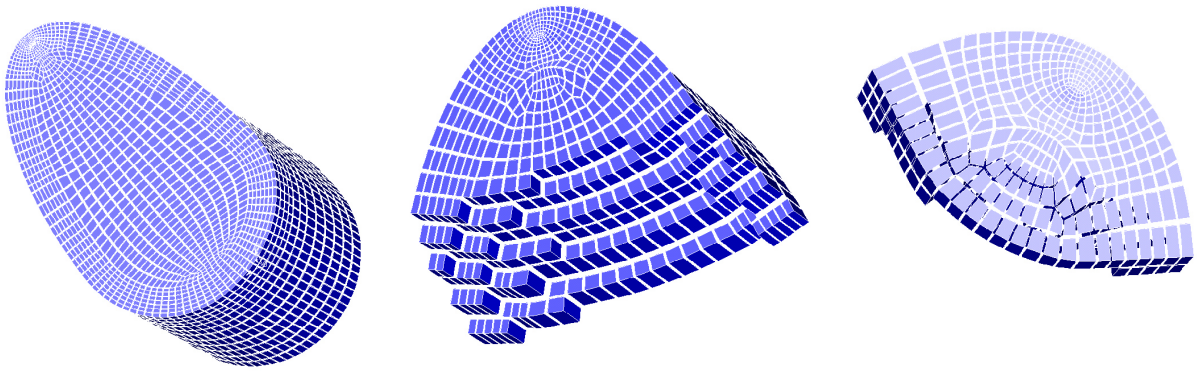

Figure 5: Different views on our hexahedral mesh with 30516 hexahedra.

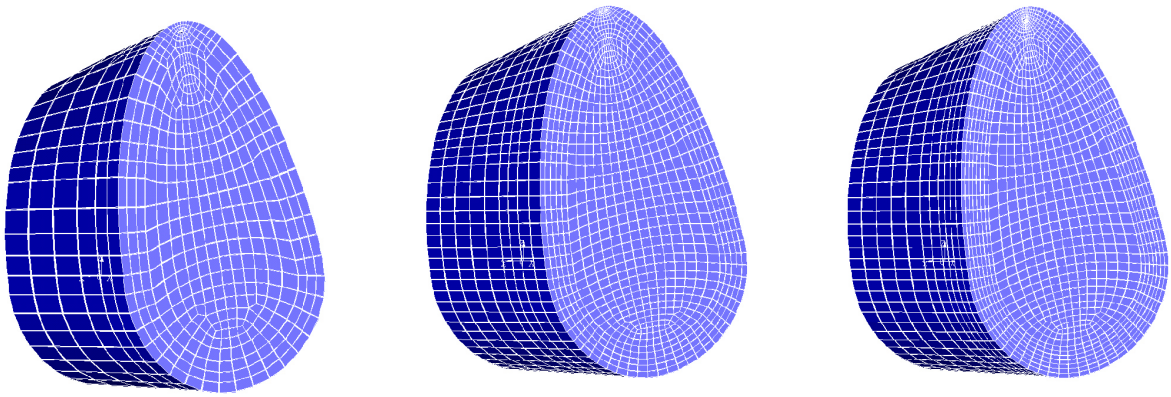

Figure 6: A “cut” through the hexahedral meshes of the piece of bone with different element size.

Average Technical Constants for the Human Mandible [AB87]											
E_1	E_2	E_3	G_{12}	G_{13}	G_{23}	ν_{12}	ν_{21}	ν_{13}	ν_{31}	ν_{23}	ν_{32}
10.8 GPa	13.3 GPa	19.4 GPa	3.81 GPa	4.12 GPa	4.63 GPa	0.309	0.381	0.249	0.445	0.224	0.328
The 1-direction is radial, the 2-direction is circumferential, and the 3-direction is axial.											

Table 1: Elastic coefficients of the human mandible.

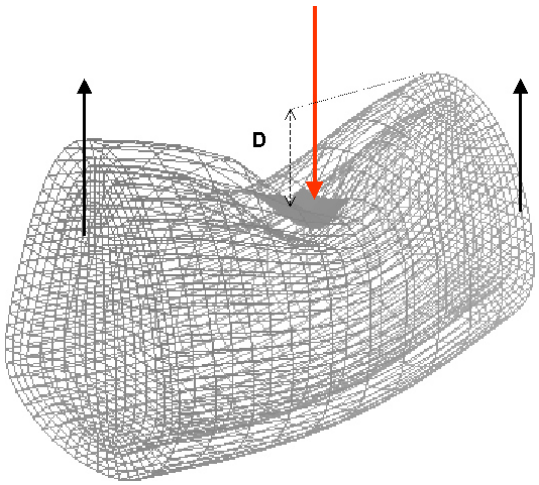

Figure 8: Deformation of the piece of bone (100 times exaggerated).

The test scenario. In our simulations, we refer to orthotropic symmetry. Based on elastomechanical coefficients coming from experiments in [AB87], see Table 1, we introduce an *index of anisotropy* α varying from isotropic material with a low Young modulus over fully anisotropic behavior again to isotropic material but with a high Young modulus, see Table 2.

We evaluated the cases with $\alpha = 0.0, 0.25$, 0.5, 0.75, 1.,1.25, 1.5, 1.75, 2.0, numbered from 1 to 9. Because of the numerical effects by at the same time a high elasticity modulus and a high Poisson-ratio, we performed additionally an isotropic simulation with $E = E_3$ and $\nu = \nu_s$ (case 10). Furthermore, we respect in every case the inhomogeneous situation given by the different material structure of cortical and cancellous bone. In [WTP], the Young modulus of spongy bone is posted as 1.29 GPa. Because we did want to keep our specimen totally anisotropic, we multiplied the Young and shear moduli of the corticalis by the factor 1.29 GPa/E_2.

For the load case, we choose a "bite like situation" where the both ends of our test specimen are elevated by masticatory forces which we realize by applied displacements of $2.0 \cdot 10^{-5} m$ (inhomogeneous Dirichlet boundary conditions), whereas at the so-called "biting point" we applied a constant force of 500 N, see Figure 8. The simulation requires the input of a force density, so we consider the quotient of this force value and the area of the biting point as applied forces (inhomogeneous Neumann or Cauchy boundary conditions). The rest of the specimen is force free, so we assume no further applied forces or displacements (homogeneous Neumann boundary conditions).

The numerical approach. In order to put all emphasis on the mesh generation especially to allow higher numbers of elements, we kept the numerics as spare as possible. Therefore, we used linear finite elements (standard shape functions with full integration, i.e., $2 \times 2 \times 2$ integration points) and refrained from higher order or hybrid approaches.

The realization of anisotropic material behavior is still a challenge in FEA. We consider orthotropic symmetry in some kind of rotated coordinate system aligned to the measurements' coordinate system in [AB87]. In order to perform the numerical calculations, we had to transform the orthotropic elasticity matrices with nine independent coefficients from its local coordinate system to the specimen's global coordinate system. By this, all the 21 independent entries of the elasticity matrix C are to be taken into account.

Because of its general flexibility, we decided to use in our simulations the research package FeliCs developed at the Chair of Applied Mathematics, Technical University of Munich [EG97].

Index of Anisotropy					
	$\alpha = 0$ isotropic	$0 < \alpha < 1$ increasing anisotropy $\nu_s = \max(\nu_{ij})$ $G_s = E_1/2(1+\nu_s)$	$\alpha = 1$ fully anisotropic	$1 < \alpha < 2$ decreasing anisotropy $\nu_h = \min(\nu_{ij})$ $G_h = E_3/2(1+\nu_h)$	$\alpha = 2$ isotropic
$E_1^{(\alpha)}$	E_1	E_1	E_1	$E_1 + (\alpha - 1) \cdot (E_3 - E_1)$	E_3
$E_2^{(\alpha)}$	E_1	$E_1 + \alpha \cdot (E_2 - E_1)$	E_2	$E_3 + (\alpha - 1) \cdot (E_2 - E_3)$	E_3
$E_3^{(\alpha)}$	E_1	$E_1 + \alpha \cdot (E_3 - E_1)$	E_3	E_3	E_3
$\nu_{ij}^{(\alpha)}$ $1 \leq i, j \leq 3$	ν_s	$\nu_s + \alpha \cdot (\nu_{ij} - \nu_s)$	ν_{ij}	$\nu_h + (\alpha - 1) \cdot (\nu_{ij} - \nu_h)$	ν_h
$G_{12}^{(\alpha)}$	G_s	$G_s + \alpha \cdot (G_{12} - G_s)$	G_{12}	$G_h + (\alpha - 1) \cdot (G_{12} - G_h)$	G_h
$G_{13}^{(\alpha)}$	G_s	$G_s + \alpha \cdot (G_{13} - G_s)$	G_{13}	$G_h + (\alpha - 1) \cdot (G_{13} - G_h)$	G_h
$G_{23}^{(\alpha)}$	G_s	$G_s + \alpha \cdot (G_{23} - G_s)$	G_{23}	$G_h + (\alpha - 1) \cdot (G_{23} - G_h)$	G_h

Table 2: Elastic coefficients depending on the index of anisotropy. For $E_1, E_2, \ldots$ see Table 1.

4 Experimental Results

4.1 Experimental Set-Up

Experiment 1: The effect of the mesh size on the solution quality. To study the dependence of the solution accuracy from the number of hexahedral elements, we varied the mesh size in the range from 5076 to 30515 hexahedra. For each mesh, we performed simulations for the ten different material scenarios.

Our mesh generation algorithms scaled well with the increasing mesh size and we could have handled much larger meshes. However, we limited the maximum size to 30515 hexahedra to keep the main memory requirements and computation times for the FEA of the whole test suite at an acceptable level.

Experiment 2: The importance of mesh quality for the solution accuracy. In our second experiment, we want to study the impact of mesh quality on the accuracy of the solution obtained in the simulation. To this end, we design an experiment which artificially degrades the mesh quality as follows. (Of course, in Experiment 1 we always take the best quality mesh for the simulation.) In a similar spirit, Freitag and Ollivier-Gooch [FOG00] have analysed the tradeoffs associated with the cost of mesh improvement in terms of solution efficiency for tetrahedral elements.

Mesh quality. There are many quality measures for hexahedral meshes, see for example [Knu00]. Here we restrict our discussion to scaled Jacobian, condition number, and the Oddy metric.

Next we give a formal definition of these metrics. Consider a vertex v of a hexahedron. Assume that $x \in \mathbb{R}^3$ is the position of this vertex and $x_i \in \mathbb{R}^3$ for $i = 1, 2, 3$ are the positions of its three neighbor vertices in some fixed order. Using edge vectors $e_i = x_i - x$ with $i = 1, 2, 3$ the Jacobian matrix is then $A = [e_1, e_2, e_3]$. The determinant of the Jacobian matrix is usually called *Jacobian*. If the edge vectors are scaled to unit length, we get the *scaled Jacobian* with values in the range -1.0 to 1.0. An element is said to be *inverted* if one of its Jacobians is less or equal to zero. In the following expressions, we use the *Frobenius matrix norm*, defined as $|A| = (tr(A^T A))^{1/2}$. The *condi-*

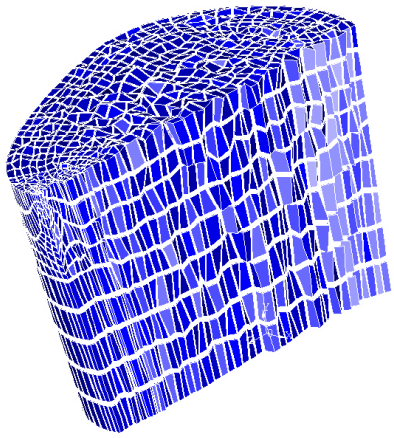

Figure 9: View on a moderately perturbed mesh.

tion number $\kappa(A)$ of A is the quantity $\kappa(A) = |A||A^{-1}|$. For the evaluation of the mesh quality, we also use another hexahedral shape measure, the so-called Oddy metric [OGMB88], which can be written in matrix form as

$$f(A) = \det(A)^{-4/3}(|A^T A|^2 - \frac{1}{3}|A|^4).$$

Construction of meshes with different mesh quality. Our construction technique to derive meshes with different levels of mesh quality is a controlled perturbation of an optimized mesh which lowers the mesh quality gradually.

Of course, we took care not to change the geometry within the perturbation process and therefore fixed the position of all nodes on the external and internal surfaces. We used an iterative procedure to move all other, non-fixed mesh nodes around. For each move, we have chosen a tentative random direction and step length. A move has been accepted if and only if it did not produce any inverted element (and so keeps the feasibility of the mesh as an invariant).

Different classes of mesh quality resulted from an increasing number of iterations over all nodes. See Figure 9 to get an impression on the degree of perturbation.

See Table 3 for the mesh quality statistics of the five different quality types used in our experiment (we display mean, standard deviation (st. dev.), and the extreme values) with 16784 hexahedra. For the interpretation, recall that the scaled Jacobian is to be maximized with an upper limit of 1.0, whereas condition number (with minimum 3.0), and the Oddy metric measure are to be minimized. Note that even the best mesh contains very poorly shaped elements. However, these extremely bad elements are only rare exceptions.

4.2 Evaluation of the experiments

In this analysis, we focus on an evaluation of the three components u, v, w of the deformation, where u and v stand for the x– resp. y–component and, w for the distance (in z–direction) of the specimen's elevated left and right-hand side ends, see Figure 8. In FEA, very often maximal values are used as indicators for practical interpretation. In our test scenario, the maxima of u, v, w are centralized on the – rather small – biting point area and so quite precisely localized. Therefore, in order to avoid tedious and maybe even falsifying interpolation procedures, we decided to compare directly the maximal values of u, v, w, see Figures 10 and 11. As, in our setting, exact solutions are not available, we consider the relative error with respect to the calculation with the finest mesh resp. the mesh with the best quality. For clarity, our plots just show the simulation results of four out of our ten cases.

Concerning the sensitivity analysis of the mesh quality, see Figure 11. In all cases, the absolute and relative dependence on the mesh quality in the considered range is relatively small. More precisely, the relative deviation from the best quality mesh is always less than four percent.

The influence of mesh size resp. number of hex elements on the solution accuracy, see Figure 10, is quite more significant. Though at a level of about 15% in the case of u or v for small meshes, the relative deviation from the largest mesh decreases steeply towards acceptable values.

One scope of this work was an analysis of the interdependence between mesh generation and inherent material law, especially in the case of anisotropy. In Figures 10 and 11, we compare two isotropic cases (case 9 and 10) with high elasticity modulus, one isotropic case with low elasticity modulus (case 1) and two anisotropic cases (case 3 and 5).

In the FEA of structural mechanics, one observes for a Poisson-ratio near 0.5 an effect called "*locking*", see [Bra97]. In this case, the stiffness matrix becomes ill-conditioned and, the calculated deformations may be much smaller than in reality. Though our highest Poisson-ratio is 0.445, see Table 1, far from locking, the related cases 1 and 10 show mostly higher relative errors than the other cases.

But, looking at the Figures 11 and 10, the most remarkable fact is, that the absolute winner of our accuracy tests, is the fully anisotropic case 5 tightly followed by the weakened anisotropic case 3. With respect to our index of anisotropy, see Table 2, we can state, that the case closest to real bone shows also the best numerical behavior. One may conjecture that the situation closest to nature has also the most balanced stress and strain pattern, and is so best

quality measure	scaled Jacobian			condition number			Oddy metric		
	min	mean	st. dev.	mean	st. dev.	max	mean	st. dev.	max
best mesh	0.06	0.96	0.08	5.63	1.76	26.38	18.1	29.46	893.9
slightly perturbed	0.06	0.92	0.08	5.84	1.84	36.60	19.5	31.32	1119.7
moderately perturbed	0.06	0.89	0.09	6.06	1.95	86.21	21.2	34.76	2113.5
strongly perturbed	0.06	0.83	0.10	6.78	2.41	149.21	26.6	44.15	4492.4
very strongly perturbed	0.06	0.76	0.11	7.94	3.29	208.80	36.9	66.55	10267.8

Table 3: Quality statistics for five test meshes with different degree of perturbation.

suited for the numerical calculation. An additional reason may be the "bite like" load case which fits quite well to the principal directions of our elasticity tensor, see Figure 7. But this load case is most similar to the physiological situation and, by this, in our setting the most important one.

We started with the question how we can "help" anisotropic numerics by appropriate meshes and end up with the insight that we have rather to adapt our meshes in the case of isotropic material law. Of course, the situation may be different if we change our load case resp. the principal directions of the elasticity tensor.

5 Conclusions

We have presented a case study on the impact of hexahedral mesh size and mesh quality on the results of a simulation in a two-material scenario with different degrees of anisotropy. Through all our experiments, the simulation results are consistent and we observed small relative errors and nice convergence properties for our meshes. Average mesh quality showed a positive, but smaller than expected impact on the solution accuracy. However, we want to stress that this does *not* mean that there is little need to smooth: without optimization-based mesh smoothing our meshes would have been invalid.

Given the inevitable sources of imprecision concerning the assumptions and simplifications of the material properties and the geometry, we conclude that it is well-justified to work with meshes with only a few thousand hexahedral elements in order to yield qualitatively meaningful results. These meshes are small enough to perform such an analysis with limited hardware resources (we used a standard PC under the linux operating system).

Our "piece of bone" turned out to be a reliable test platform which can be used for further maybe more material oriented evaluations.

Future work. Subsequent work should address a couple of further issues.

1. This paper has focused on accuracy and convergence with respect to the mesh size and to the mesh quality. A natural extension would be to study the costs or benefits on solution efficiency.

2. In this analysis, we restricted ourselves to a relatively simple numerical approach. Can we draw similar conclusions if we use more advanced numerical concepts? For example, one could use 20-node brick elements with reduced integration to get rid of the locking phenomena.

3. We concentrated our analysis on the maximum deformation as indicator for the solution accuracy. Do we get the same picture if we consider other post-processing variables like von Mises equivalent stress, volumetric strain, and principal shear strain?

4. Would other load cases produce other results concerning the interdependence of required mesh size and quality and the material law?

5. Finally, one would like to perform a rigorous comparison between hex and tet meshing.

Acknowledgments. The authors want to thank K.–H. Hoffmann, caesar foundation Bonn, for the possibility to use the FEM–package FeliCs, and also N.D. Botkin for his help concerning its compilation.

The second author wants to thank I.G. Götz for his appreciated advice concerning FeliCs which made the necessary source code extensions for the anisotropic calculations possible. Finally, the authors wish to thank G. Krause for providing us with the finite element preprocessor ISAGEN (which we used for our illustrations).

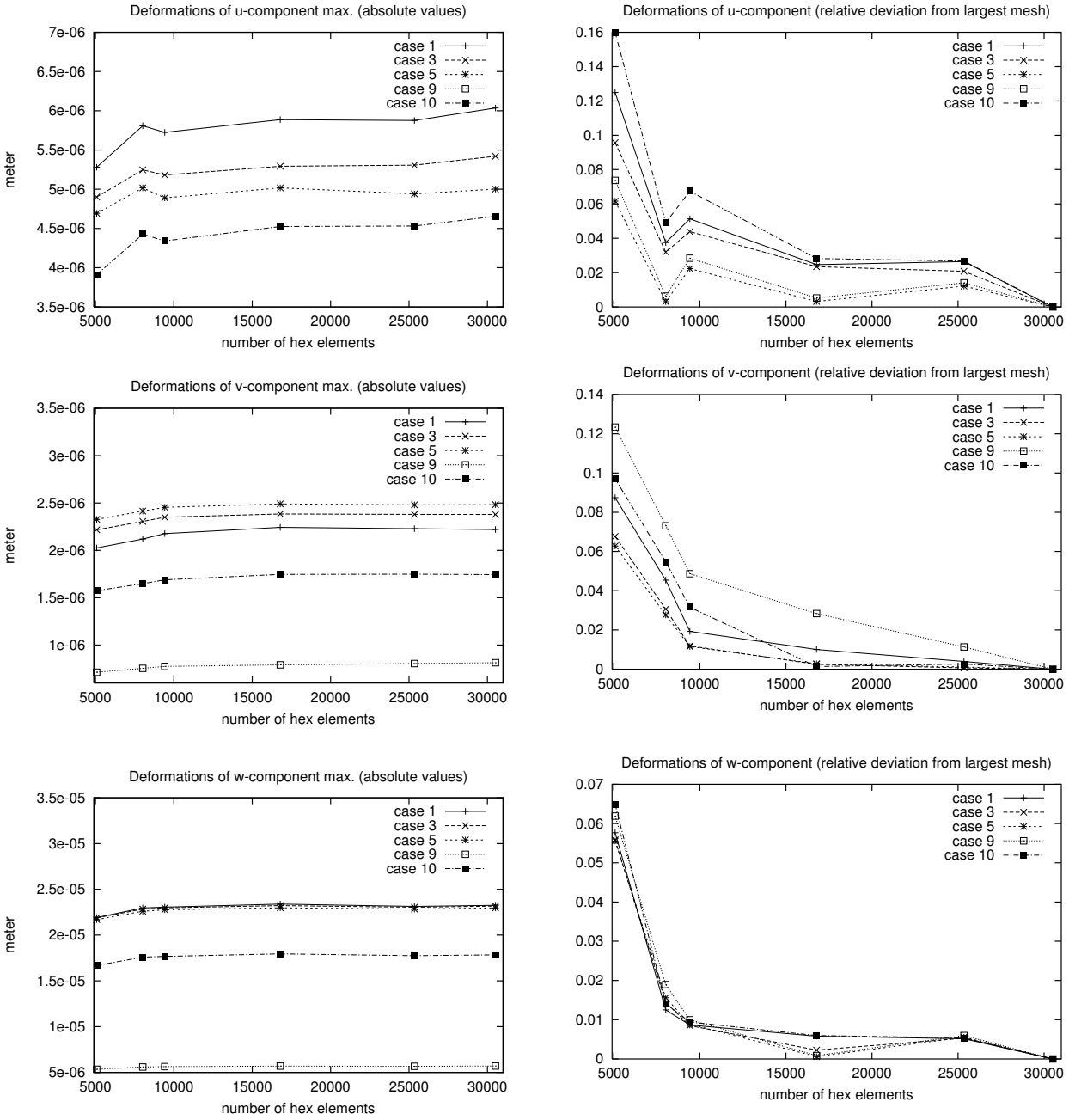

Figure 10: Evaluation of the deformation versus number of hex elements.

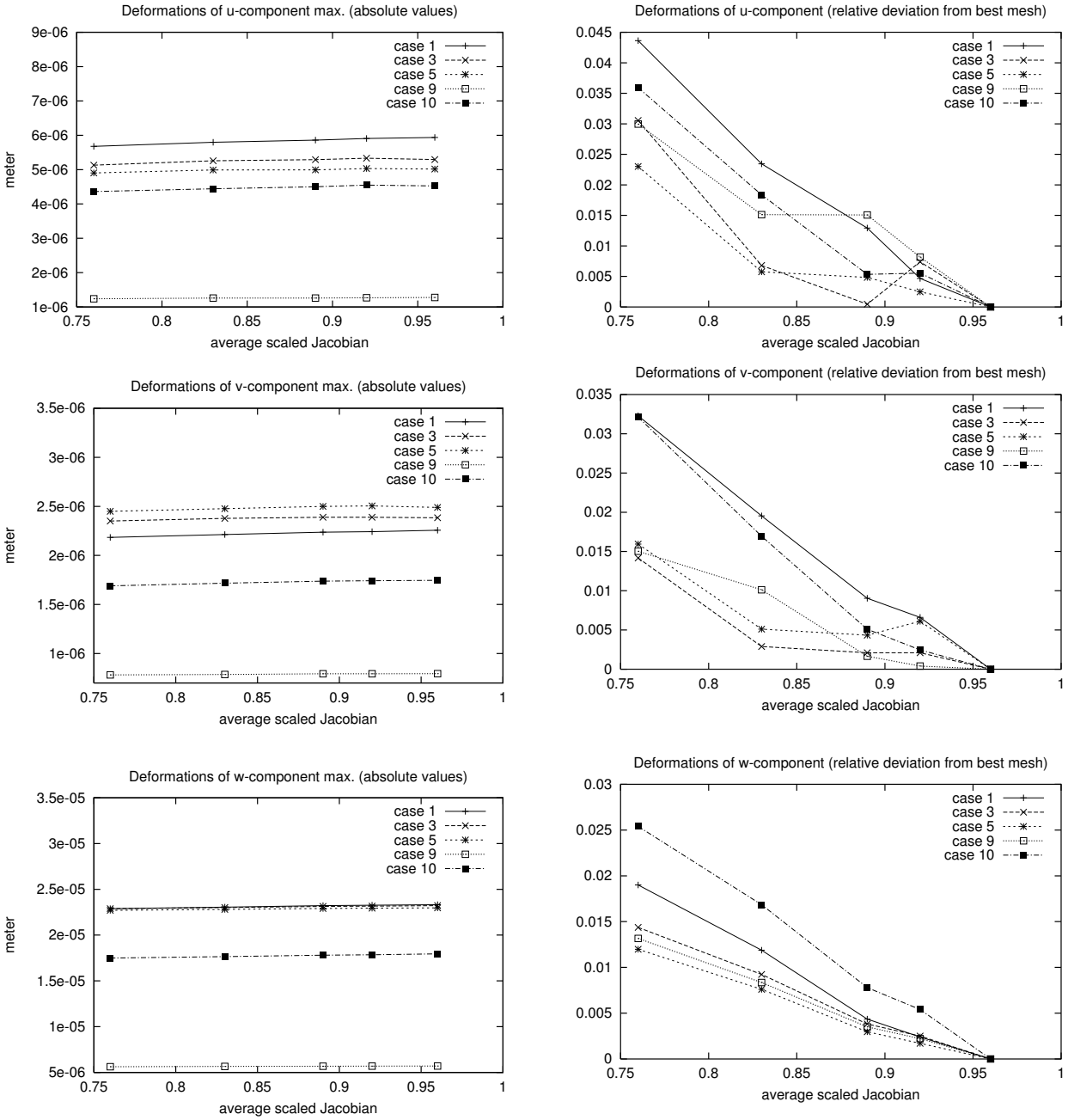

Figure 11: Evaluation of the deformation versus hex mesh quality for test meshes with 16784 elements.

References

[AB87] R.B. Ashman and W.C. Van Buskirk, *The elastic properties of a human mandible*, Adv. Dent. Res. **1** (1987), 64–67.

[Bra97] D. Braess, *Finite elements: Theory, fast solvers and applications in solid mechanics*, Cambridge University Press, 1997.

[Daw76] T. H. Dawson, *Theory and practice of solid mechanics*, Plenum Press, New York, 1976.

[EG97] I. Eichenseher and I. G. Götz, *FeliCs — internal documentation*, Tech. report, Chair of Applied Mathematics, University of Technology Munich, 1997.

[FK99] L. A. Freitag and P. M. Knupp, *Tetrahedral element shape optimization via the jacobian determinant and condition number*, Proceedings of the 8th International Meshing Roundtable, South Lake Tahoe, CA, Sandia National Laboratories, Albuquerque, USA, 1999, pp. 247–258.

[FOG00] L. A. Freitag and C. Ollivier-Gooch, *A cost/benefit analysis of simplicial mesh improvement techniques as measured by solution efficiency*, International Journal of Computational Geometry and Applications **10** (2000), 361–382.

[KBZ+00] C. Kober, H.-J. Bauer, H.-F. Zeilhofer, K.-H. Hoffmann, R. Sader, H. Thiele, H. Deppe, and U. Kliegis, *FEM simulation of the human mandible: a preliminary step for new osteosynthesis techniques*, Proceedings of Euromat99 — "Materials for Medical Engineering" (H. Stallforth, ed.), Wiley-VCH, 2000.

[KMH01] C. Kober and M. Müller-Hannemann, *A case study in hexahedral mesh generation: Simulation of the human mandible*, Engineering with Computers (2001), to appear.

[Knu00] P. M. Knupp, *Achieving finite element mesh quality via optimization of the jacobian matrix norm and associated quantities, part II — a framework for volume mesh optimization*, Int. J. Numer. Methods in Eng. **48** (2000), 1165–1185.

[KST+00] C. Kober, R. Sader, H. Thiele, H.-J. Bauer, H.-F. Zeilhofer, K.-H. Hoffmann, and H.-H. Horch, *A modular software concept for the individual numerical simulation (fem) of the human mandible*, Biomedizinische Technik **45** (2000), 119–125.

[MBS98] R. B. Martin, D. B. Burr, and N. A. Sharkey, *Skelatal tissue mechanics*, Springer-Verlag, New York Berlin Heidelberg, 1998.

[MH99] M. Müller-Hannemann, *Hexahedral mesh generation by successive dual cycle elimination*, Engineering with Computers **15** (1999), 269–279.

[MH01] M. Müller-Hannemann, *Improving the surface cycle structure for hexahedral mesh generation*, Computational Geometry Theory and Applications (2001), to appear.

[MM00] R. H. Möhring and M. Müller-Hannemann, *Complexity and modeling aspects of mesh refinement into quadrilaterals*, Algorithmica **26** (2000), 148–171.

[OGMB88] A. Oddy, J. Goldak, M. McDill, and M. Bibby, *A distortion metric for isoparametric finite elements*, Trans. CSME, No. 38-CSME-32, Accession No. 2161 (1988).

[PP94] R. Putz and R. Pabst, *Sobotta atlas of human anatomy*, Urban & Schwarzenberg, Munich, Vienna, Baltimore, 1994.

[Tau01] T. J. Tautges, *The generation of hexahedral meshes for assembly geometry: survey and progress*, International Journal for Numerical Methods in Engineering **50** (2001), 2617–2642.

[VO00] H. Van Oosterwyck, *Study of biomechanical determinants of bone adaptation around functionally loaded oral implants*, Ph.D. thesis, Katholieke Universiteit Leuven, Faculteit Toegepaste Wetenschappen, Department Werktuigkunde Afdeling Biomechanica en Grafisch Ontwerpen, 2000.

[WTP] G.E.O. Widera, J.A. Tesk, and E. Priviter, *Interaction effects among cortical bone, cancellous bone and peridontal membrane of natural teeth and implants*, J. Biomed. Matre. Res. Symp. **7**, 613–623.